Table II. Constants of Tait Equation for Liquid Ammonia

Temp, °C	B, atm	C
−20	1336.8	0.1101
0	1036.4	
25	714.4	
40	567.1	

To ascertain the applicability of the new piezometer, the compression of benzene was measured at 25° C, since it had been accurately determined by Gibson and Kincaid (5) and by Bett et al. (3). The values of compression obtained by the present work are 0.03256 at 405.7 bar and 0.05658 at 811.4 bar, which are satisfactorily close to the values 0.03237 (3), 0.03262 (5) at 405.7 bar, and 0.05634 (3), 0.05678 (5) at 811.4 bar, respectively.

RESULTS

The experimental specific volumes of liquid ammonia at −20°, 0°, 25°, and 40° C up to 1800 atm are shown in Table I and in Figure 4. All points lie on a smooth curve with deviations less than 0.13% over the whole range of measurements. The values of specific volumes at the saturated pressures obtained by extrapolation agree with those presented in the International Critical Tables (7). The values obtained by Keyes (8), Tsiklis (9), and Date and Iwasaki (4) are included in Figure 4 for comparison with the present results. The present results at 25° C below 900 atm agree with those obtained by Date and Iwasaki and by Keyes within experimental accuracy, but the values above 900 atm differ from those by Keyes. The present data are consistently higher at 40° C and lower at 0° C than those of Keyes.

The Tait equation (6),

$$V_p = V_0\{1 - C \ln [(B + p)/(B + p_0)]\} \qquad (2)$$

has been found to describe most of the isothermal data. The constants of this equation were calculated by means of the method of least squares with the present data. Table II gives the values of B and C for liquid ammonia at four temperatures. The specific volume at the saturated pressure (7) was chosen as V_0.

The standard errors of the experimental values from those calculated by the Tait equation are 0.05, 0.02, 0.03, and 0.07% at −20°, 0°, 25°, and 40° C, respectively.

ACKNOWLEDGMENT

The authors wish to express their sincere thanks to Hiroji Iwasaki, Shinji Takahashi, and Kaoru Date for their kind advice throughout this work.

NOMENCLATURE

a = cross-sectional area of capillary tube, cm^2
B, C = constants of Tait equation (2)
k = compression of borosilicate glass, 1/atm
l = length from mark to lower end of indicator, cm
m = mass of liquid, gram
n = number of data
p_0, p = pressures, atm
t = temperature, °C
v_0 = volume of glass bulb above mark, cm^3
v_1 = volume of indicator, cm^3
v_2 = volume of liquid occupying space between capillary tube wall and float, cm^3
V_{calcd}, V_{exptl} = specific volumes calculated by Tait equation and experimental one, respectively, cm^3/gram
V_0, V_p = specific volumes at pressures p_0 and p atm, respectively, cm^3/gram
α = cubic expansion coefficient of borosilicate glass, 1/°C

LITERATURE CITED

(1) Adams, L. H., *J. Amer. Chem. Soc.*, **53**, 3769 (1931).
(2) Adams, L. H., Gibson, R. E., *J. Wash. Acad. Sci.*, **21**, 381 (1931).
(3) Bett, K. E., Hayes, P. F., Newitt, D. M., *Phil. Trans. Roy. Soc. London*, **Ser. A923** (247), 59 (1954).
(4) Date, K., Iwasaki, H., Preprint of the 9th Symposium on High Pressure, Nagoya, Japan, p 105, 1967.
(5) Gibson, R. E., Kincaid, J. F., *J. Amer. Chem. Soc.*, **60**, 511 (1938).
(6) Hirschfelder, J. O., Curtiss, C. F., Bird, R. B., "Molecular Theory of Gases and Liquids," Wiley, New York, N. Y., 1954.
(7) "International Critical Tables," Vol. III, p 234, McGraw-Hill, New York, N. Y., 1928.
(8) Keyes, F. G., *J. Amer. Chem. Soc.*, **53**, 965 (1931).
(9) Tsiklis, D. S., *Dokl. Acad. Nauk SSSR*, **91**, 889 (1953).
(10) Kumagai, A., Date, K., *Bull. Chem. Res. Inst. Non-Aq. Sol.*, Tohoku Univ., Japan, **19**, 149 (1969).

RECEIVED for review April 14, 1970. Accepted December 20, 1970.

Phase Equilibrium of Carbon Dioxide and Light Paraffins in Presence of Solid Carbon Dioxide

UN K. IM[1] and FRED KURATA[2]
Center for Research in Engineering Science, University of Kansas, Lawrence, Kan. 66044

Cryogenic processes for separation of hydrocarbons from natural gas can be designed to operate as close to the freezing point of the feed stream as desired, providing the solubility limit of carbon dioxide in hydrocarbons is not exceeded. Carbon dioxide in excess of its solubility limit would precipitate out as a solid due to its relatively high triple point compared to hydrocarbons.

[1] Present address, Process Design & Economics, Organic Chemicals Division, Amoco Chemicals Corp., Naperville, Ill. 60540.
[2] To whom correspondence should be addressed.

At the limit of saturated condition, the vapor-liquid equilibrium relationship, commonly represented by molal equilibrium ratios, should approach that of the solid-liquid-vapor equilibrium where the solid phase is pure carbon dioxide.

During experimental studies of the solubility of carbon dioxide in multicomponent hydrocarbon systems (3), equilibrium vapor and liquid compositions were determined to evaluate molal equilibrium ratios of hydrocarbons and carbon dioxide along the solid-liquid-vapor loci in the following systems:

Molal equilibrium ratios (*K* values) for hydrocarbons and carbon dioxide were evaluated for multicomponent hydrocarbon systems containing methane, ethane, propane, and *n*-butane, saturated with carbon dioxide at temperatures below the triple point of carbon dioxide. Temperature measurement was accurate to ±0.3° F, and pressure was measured to an accuracy of ±0.5 psia. The maximum relative uncertainty estimated from statistical analysis of the chromatograph calibration data was ±3.2% for composition given in mole fractions or ±7.4% for molal equilibrium ratios reported. In general, molal equilibrium ratios for methane and carbon dioxide are affected very little by the nature or concentration of heavier hydrocarbons present in the system. Molal equilibrium ratios for hydrocarbons in the presence of solid carbon dioxide are invariably higher than those of hydrocarbon systems without carbon dioxide at the same temperature and pressure range at temperatures above −100° F.

Ternary Systems
- Carbon dioxide–methane—propane
- Carbon dioxide–methane–*n*-butane
- Carbon dioxide–ethane–propane

Quaternary System
- Carbon dioxide–methane–ethane–propane

In addition, molal equilibrium ratios were evaluated for carbon dioxide–methane–ethane system based on the data provided by Jensen (*4*) and for carbon dioxide–methane system from the study of Davis et al. (*2*) and Brewer and Kurata (*1*).

EXPERIMENTAL PROCEDURE

A detailed description of the experimental equipment and procedure is given elsewhere (*3*). Briefly, phase compositions along solid-liquid-vapor loci were determined by analyzing phase samples withdrawn from an equilibrium cell maintained at the specified equilibrium conditions. Constant temperatures were provided in an air bath using liquid nitrogen as the refrigerant. The bath temperature was measured by a platinum resistance thermometer calibrated against a secondary standard. Although the calibration accuracy of the thermometer was better than ±0.1° F, the maximum uncertainty for temperature measurement was given as ±0.3° F due to a small thermal gradient in the bath. Pressure was measured by a Heise gage and its accuracy was ±0.5 psia as determined by calibration against a laboratory standard transfer gage (Seager gage). Phase samples were analyzed on a F&M 720 gas chromatograph and the maximum relative uncertainty for composition reported was estimated to be ±3.2% (*3*). Hydrocarbons used were research grades furnished by Phillips Petroleum Co. and carbon dioxide used was Coleman grade obtained from Matheson gas products. Stated purity for all fluids used was 99.9+ mol %, and subsequent analysis confirmed this claimed purity.

According to the phase rule, the number of degrees of freedom for solid-liquid-vapor equilibria is reduced by one as compared to vapor-liquid equilibria. Thus a ternary system has two degrees of freedom to fix the equilibrium state completely. In addition to temperature, a composition variable defined as the composition of hydrocarbon on a carbon dioxide-free basis in the liquid phase was chosen as the second variable. In practice, a mixture of hydrocarbons of predetermined ratio was prepared in a stainless steel reservoir in the charging manifold. Although unequal vaporization constants for hydrocarbons produce variations in liquid composition parameter, ϕ, defined as the mole fraction of the lighter of two heavier hydrocarbons present on a methane- and carbon dioxide-free basis, its effect on molal equilibrium ratios was found to negligible.

In the quaternary system, the number of degrees of freedom is three. The variables to be specified in addition to temperature were chosen as the composition parameter, ϕ, defined above, and pressure. The adjustment of pressure was easily accomplished by metering methane into the equilibrium cell in small quantities by means of a manual positive displacement pump located in the charging manifold.

Ranges of variables investigated are listed below:

Carbon dioxide–methane–propane system
- Temperatures: −84.9°, −90.3°, −99.3°, −126.3°, −162.3°, −189.3° F
- Composition parameters: 0.35, 0.65

Carbon dioxide–methane–*n*-butane system
- Temperatures: −81.3, −84.9, −90.3, −126.3° F
- Composition parameters: 0.35, 0.60, 0.75

Carbon dioxide–ethane–propane system
- Temperatures: −84.9, −90.3, −99.3, −117.3° F
- Composition parameters: 0.35; 0.65

Carbon dioxide–methane–ethane–propane system
- Temperatures: −84.9, −90.3, −99.3, −117.3° F
- Pressures: 200, 300, 400 psia
- Composition parameters: 0.28, 0.68

EXPERIMENTAL RESULTS

Vapor and liquid compositions and calculated molal equilibrium ratios are given in Tables I through V for four ternary and one quaternary systems studied by Jensen (*4*) and this work. In addition, high-pressure terminal points of methane isotherms are given by carbon dioxide–methane system molal equilibrium ratios, and they were evaluated from data reported by Davis et al. (*2*) and Brewer and Kurata (*1*) and are summarized in Table VI.

Molal equilibrium ratios of methane when plotted against pressure on log-log scales as shown in Figure 1 can be represented by straight lines passing through carbon dioxide–methane binary system limits. Each isotherm in Figure 1 is the best line through the data points at each temperature for all the systems studied. Figure 1 shows that the molal equilibrium ratio of methane in different systems is approximately the same at a given temperature and pressure regardless of what other heavier hydrocarbons are present in the system. Thus, although data points show some scatter, particularly at higher pressures, the effect of heavier components on the methane molal equilibrium ratios may be safely discounted.

Figure 2 shows molal equilibrium ratios for carbon dioxide in ternary systems. Here, also, the effect of heavy hydrocarbons on molal equilibrium ratios is insignificant. Molal equilibrium ratios for carbon dioxide in the quaternary system are shown in Figure 3.

Molal equilibrium ratios for hydrocarbons in the quaternary system are compared in Figures 4 and 5 with the corresponding values of the ternary systems of hydrocarbons alone. Differences are rather striking. At −117.3° F, the lowest isotherm, molal equilibrium ratios for hydrocarbons with or without carbon dioxide present are practically identical. However, at successively higher temperatures, molal equilibrium ratios along the solid-liquid-vapor locus are

Table I. Molal Equilibrium Ratios along S-L-V Locus in Carbon Dioxide–Methane–Ethane System[a]

T, °F	P, psia	Liquid composition, mole fraction			Vapor composition, mole fraction			Molal equilibrium ratio			$C_1/(C_1 + C_2) = \phi$
		CO_2	CH_4	C_2H_6	CO_2	CH_4	C_2H_6	CO_2	CH_4	C_2H_6	
−84.9	269.5	0.6361	0.1553	0.2086	0.1889	0.7224	0.0887	0.297	4.652	0.425	0.427
−84.9	418.3	0.6446	0.2439	0.1115	0.1421	0.8152	0.0427	0.220	3.342	0.383	0.686
−89.9	281.4	0.4980	0.2154	0.2866	0.1567	0.7522	0.0911	0.315	3.492	0.318	0.429
−89.9	442.2	0.4753	0.3680	0.1567	0.1168	0.8413	0.0419	0.246	2.286	0.267	0.701
−100.0	275.6	0.3188	0.2936	0.3878	0.0914	0.8254	0.0832	0.287	2.811	0.215	0.431
−100.0	436.2	0.2908	0.4896	0.2196	0.0675	0.8902	0.0423	0.232	1.818	0.193	0.690
−129.9	205.5	0.1015	0.3863	0.5122	0.0297	0.9146	0.0557	0.293	2.368	0.109	0.430
−129.9	330.5	0.0914	0.6364	0.2722	0.0192	0.9589	0.0219	0.210	1.507	0.080	0.700
−159.9	130.9	0.0384	0.4022	0.5594	0.0105	0.9575	0.0320	0.273	2.381	0.057	0.418
−159.9	200.5	0.0336	0.6732	0.2932	0.0087	0.9767	0.0146	0.259	1.451	0.050	0.697

[a] Vapor-liquid composition data from Jensen (*4*).

Table II. Molal Equilibrium Ratios along S-L-V Locus in Carbon Dioxide–Methane–Propane System

T, °F	P, psia	Liquid composition, mole fraction			Vapor composition, mole fraction			Molal equilibrium ratio			$C_1/(C_1 + C_3) = \phi$
		CO_2	CH_4	C_3H_8	CO_2	CH_4	C_3H_8	CO_2	CH_4	C_3H_8	
−84.9	205.5	0.5975	0.1396	0.2628	0.2026	0.7794	0.0180	0.338	5.583	0.068	0.347
−84.9	320.5	0.6201	0.2120	0.1679	0.1592	0.8303	0.0105	0.257	3.917	0.063	0.558
−90.3	199.5	0.4320	0.1630	0.4050	0.1765	0.8043	0.0192	0.409	4.934	0.047	0.287
−90.3	343.0	0.4595	0.2919	0.2486	0.1247	0.8620	0.0124	0.271	2.956	0.050	0.540
−99.3	148.5	0.2633	0.2181	0.5185	0.1112	0.8720	0.0168	0.422	3.998	0.032	0.296
−99.3	339.0	0.2613	0.3713	0.3674	0.0756	0.9142	0.0101	0.289	2.462	0.027	0.503
−126.3	167.0	0.1094	0.2635	0.6271	0.0472	0.9497	0.0072	0.431	3.604	0.011	0.296
−126.3	306.5	0.1051	0.5277	0.3672	0.0269	0.9688	0.0044	0.256	1.836	0.012	0.590
−162.3	110.0	0.0332	0.3157	0.6511	0.0126	0.9848	0.0027	0.380	3.119	0.004	0.327
−162.3	192.0	0.0292	0.6334	0.3374	0.0069	0.9919	0.0013	0.236	1.566	0.004	0.653
−189.3	66.3	0.0108	0.3278	0.6614	0.0040	0.9944	0.0015	0.370	3.034	0.002	0.331
−189.3	110.0	0.0103	0.6418	0.3479	0.0025	0.9969	0.0006	0.243	1.553	0.002	0.649

Table III. Molal Equilibrium Ratios along S-L-V Locus in Carbon Dioxide–Methane–*n*-Butane System

T, °F	P, psia	Liquid composition, mole fraction			Vapor composition, mole fraction			Molal equilibrium ratio			$C_1/(C_1 + C_4) = \phi$
		CO_2	CH_4	n-C_4H_{10}	CO_2	CH_4	n-C_4H_{10}	CO_2	CH_4	n-C_4H_{10}	
−81.3	192.0	0.6797	0.0927	0.2277	0.2888	0.7090	0.0022	0.425	7.648	0.010	0.289
−81.3	340.0	0.7486	0.1622	0.0892	0.1829	0.8157	0.0014	0.244	5.029	0.016	0.645
−81.3	451.0	0.7812	0.1934	0.0254	0.1388	0.8605	0.0008	0.178	4.449	0.031	0.884
−84.9	208.5	0.5461	0.1430	0.3109	0.2213	0.7767	0.0020	0.405	5.431	0.006	0.315
−84.9	374.0	0.6325	0.2322	0.1353	0.1415	0.8566	0.0018	0.224	3.689	0.006	0.632
−84.9	483.0	0.6351	0.2813	0.0836	0.1178	0.8811	0.0011	0.185	3.132	0.013	0.771
−90.3	226.0	0.3916	0.1776	0.4308	0.1731	0.8246	0.0023	0.442	4.643	0.005	0.292
−90.3	369.0	0.4560	0.3113	0.2327	0.1211	0.8775	0.0015	0.266	2.819	0.006	0.847
−90.3	466.5	0.4448	0.4165	0.1387	0.0729	0.9259	0.0012	0.164	2.223	0.009	0.750
−126.3	185.0	0.1137	0.2508	0.6355	0.0384	0.9597	0.0019	0.338	3.827	0.003	0.283
−126.3	358.0	0.1048	0.5601	0.3351	0.0255	0.9737	0.0008	0.243	1.738	0.002	0.626
−99.3	227.5	0.2504	0.2109	0.5387	0.1272	0.8700	0.0028	0.508	4.125	0.005	0.281
−99.3	372.0	0.2953	0.3867	0.3180	0.0768	0.9221	0.0010	0.260	2.385	0.003	0.549

Table IV. Molal Equilibrium Ratios along S-L-V Locus in Carbon Dioxide–Ethane–Propane System

T, °F	P, psia	Liquid composition, mole fraction			Vapor composition, mole fraction			Molal equilibrium ratio			$C_2/(C_2 + C_3) = \phi$
		CO_2	C_2H_6	C_3H_6	CO_2	C_2H_6	C_3H_8	CO_2	C_2H_6	C_3H_8	
−84.9	56.5	0.5774	0.1455	0.2772	0.7766	0.1817	0.0417	1.345	1.249	0.150	0.344
−84.9	67.0	0.6320	0.2637	0.1043	0.6665	0.3127	0.0208	1.055	1.186	0.199	0.717
−90.3	48.0	0.4141	0.2070	0.3789	0.7437	0.2095	0.0468	1.796	1.012	0.124	0.353
−90.3	58.5	0.4655	0.3981	0.1364	0.6226	0.3612	0.0161	1.337	0.907	0.118	0.745
−99.3	35.0	0.2593	0.2782	0.4626	0.6877	0.2620	0.0503	2.652	0.942	0.109	0.376
−99.3	44.0	0.2823	0.5150	0.2027	0.5558	0.4223	0.0219	1.969	0.820	0.108	0.717
−117.3	17.5	0.1183	0.3364	0.5453	0.5764	0.3634	0.0602	4.872	1.080	0.110	0.382
−117.3	24.0	0.1320	0.6372	0.2309	0.4430	0.5328	0.0243	3.356	0.836	0.105	0.734

Table V. Molar Equilibrium Ratios along S-L-V Locus in Carbon Dioxide–Methane–Ethane–Propane System

T, °F	P, psia	Liquid composition, mole fraction				Vapor composition, mole fraction				Molal equilibrum ratio				$C_2/(C_2+C_3)=\phi$
		CO_2	CH_4	C_2H_6	C_3H_8	CO_2	CH_4	C_3H_6	C_3H_8	CO_2	CH_4	C_3H_6	C_3H_8	
−84.9	300.0	0.6566	0.1761	0.0424	0.1249	0.1676	0.8036	0.0188	0.0100	0.255	4.563	0.443	0.080	0.254
−84.9	400.0	0.6455	0.2408	0.0289	0.0848	0.1419	0.8394	0.0117	0.0070	0.220	3.486	0.405	0.083	0.255
−90.3	200.0	0.4584	0.1541	0.0876	0.2999	0.1910	0.7623	0.0304	0.0163	0.417	4.947	0.347	0.054	0.226
−90.3	300.0	0.4888	0.2381	0.0676	0.2055	0.1366	0.8340	0.0202	0.0092	0.279	3.503	0.299	0.045	0.244
−90.3	400.0	0.4969	0.3240	0.0452	0.1339	0.1170	0.8623	0.0132	0.0075	0.235	2.661	0.292	0.056	0.253
−99.3	200.0	0.3025	0.1964	0.1291	0.3720	0.1322	0.8232	0.0309	0.0127	0.437	4.191	0.239	0.034	0.257
−99.3	300.0	0.3095	0.3102	0.0958	0.2845	0.0956	0.8765	0.0190	0.0089	0.309	2.826	0.198	0.031	0.252
−99.3	400.0	0.3097	0.4278	0.0625	0.2000	0.0724	0.9103	0.0110	0.0063	0.234	2.128	0.176	0.032	0.238
−117.3	200.0	0.1477	0.2734	0.1636	0.4153	0.0605	0.9068	0.0237	0.0090	0.234	3.317	0.145	0.022	0.283
−117.3	300.0	0.1673	0.4301	0.1102	0.2924	0.0445	0.9360	0.0138	0.0057	0.266	2.176	0.125	0.019	0.273
−84.9	300.0	0.6430	0.1755	0.1224	0.0591	0.1652	0.7783	0.0519	0.0046	0.257	4.435	0.424	0.078	0.675
−84.9	400.0	0.6741	0.2242	0.0686	0.0591	0.1652	0.8581	0.0300	0.0030	0.162	3.827	0.437	0.091	0.750
−90.3	200.0	0.4829	0.1438	0.2520	0.1203	0.2026	0.6903	0.0998	0.0073	0.420	4.800	0.396	0.061	0.679
−90.3	300.0	0.5047	0.2315	0.1768	0.0870	0.1399	0.8006	0.0550	0.0045	0.277	3.458	0.311	0.052	0.725
−90.3	400.0	0.4976	0.3200	0.1225	0.0599	0.1198	0.8404	0.0365	0.0033	0.241	2.626	0.298	0.055	0.672
−99.3	200.0	0.3202	0.1874	0.3350	0.1573	0.1348	0.7751	0.0847	0.0054	0.421	4.136	0.253	0.034	0.680
−99.3	300.0	0.3136	0.3188	0.2533	0.1143	0.0969	0.8466	0.0528	0.0037	0.309	2.656	0.208	0.032	0.690
−99.3	400.0	0.3151	0.4147	0.1774	0.0828	0.0884	0.8690	0.0391	0.0035	0.281	2.095	0.220	0.042	0.682
−117.3	200.0	0.1522	0.2884	0.3780	0.1814	0.0613	0.8746	0.0613	0.0028	0.403	3.033	0.162	0.015	0.678
−117.3	300.0	0.1530	0.4447	0.2749	0.1274	0.0371	0.9245	0.0364	0.0020	0.242	2.079	0.132	0.016	0.684

Table VI. Molal Equilibrium Ratios along S-V-L Locus in Carbon Dioxide–Methane System[a]

T, °F	P, psia	Liquid composition, mole fraction		Vapor composition, mole fraction		Molal equilibrium ratio	
		CO_2	CH_4	CO_2	CH_4	CO_2	CH_4
−81.3	580.0	0.7400	0.2600	0.1750	0.8250	0.236	3.170
−84.9	655.0	0.6500	0.3500	0.1500	0.8500	0.231	2.300
−89.9	702.0	0.4300	0.5700	0.1130	0.8870	0.263	1.560
−90.3	703.0	0.3450	0.6550	0.1110	0.8890	0.322	1.360
−99.3	695.0	0.2070	0.7930	0.0780	0.9220	0.383	1.160
−100.0	690.0	0.1970	0.8030	0.0760	0.9340	0.386	1.150
−117.3	577.0	0.0970	0.8780	0.0413	0.9220	0.426	1.092
−126.3	510.0	0.0710	0.9260	0.0300	0.9700	0.422	1.050
−159.9	287.0	0.0355	0.9665	0.0140	0.9860	0.418	1.020
−162.3	275.0	0.0183	0.9817	0.0060	0.9940	0.327	1.013

[a] Based on data of Davis et al. (2).

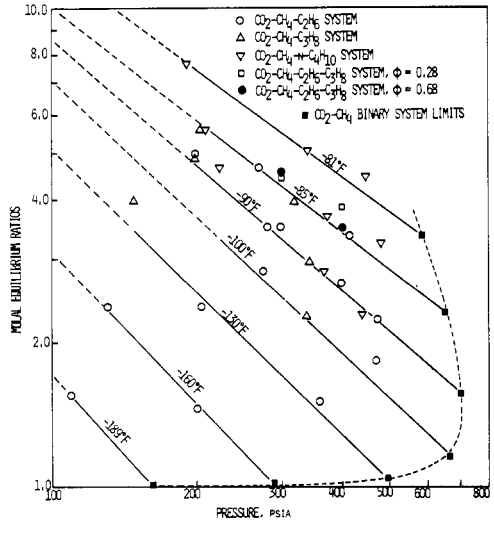

Figure 1. Molal equilibrium ratios for methane in carbon dioxide–hydrocarbon systems

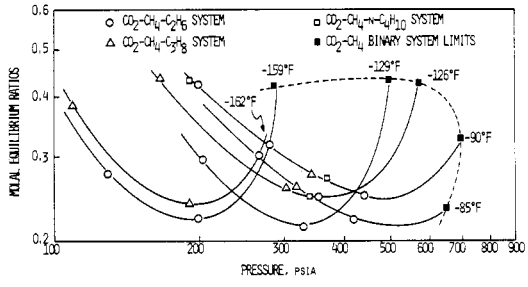

Figure 2. Molal equilibrium ratios for carbon dioxide in carbon dioxide–hydrocarbon ternary systems

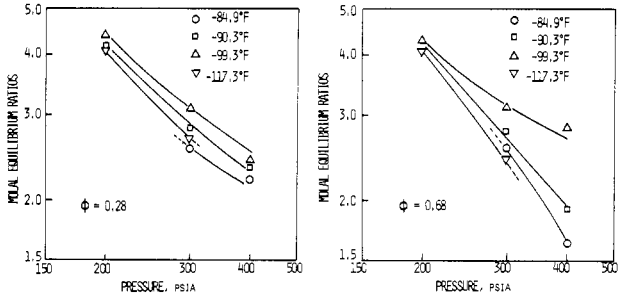

Figure 3. Molal equilibrium ratios for carbon dioxide in carbon dioxide–methane–ethane–propane system

invariably higher than those of vapor-liquid equilibrium, and the difference becomes greater with the increasing temperature. Furthermore, for methane, log K vs. T curves actually show a reversed curvature. Another difference is that, whereas the pressure effect on molal equilibrium ratios in vapor-liquid equilibrium tends to be greater at higher temperature, the opposite effect is true when carbon dioxide is present as a solid.

In Figures 3, 4, and 5, ϕ is the composition parameter previously defined.

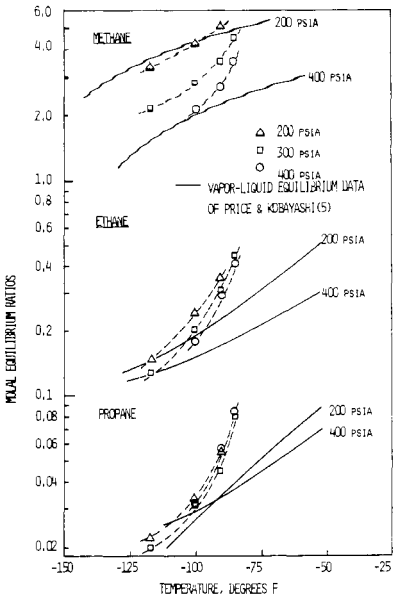

Figure 4. Molal equilibrium ratios for hydrocarbons in carbon dioxide–methane–ethane–propane system at ϕ = 0.28

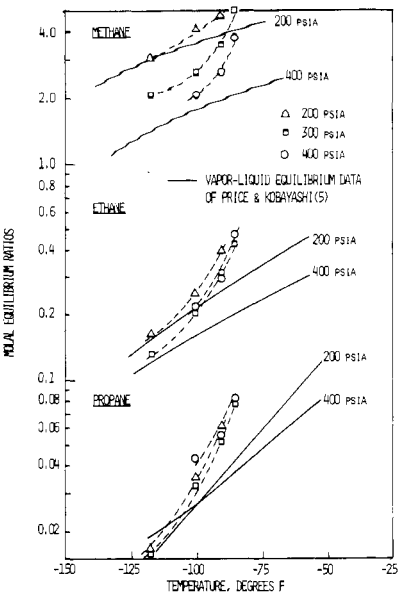

Figure 5. Molal equilibrium ratios for hydrocarbons in carbon dioxide–methane–ethane–propane system at ϕ = 0.68

ACKNOWLEDGMENT

The authors are grateful to Phillips Petroleum Company for their donation of hydrocarbons and to the Computation Center of the University of Kansas for allocation of computer time for this project.

LITERATURE CITED

(1) Brewer, J., Kurata, F., *AIChE J.*, **4**, 317 (1958).
(2) Davis, J. A., Rodewald, N., Kurata, F., *ibid.*, **8**, 537 (1962).
(3) Im, U. K., "Solubility of Solid Carbon Dioxide in Certain Paraffinic Hydrocarbons: Binary, Ternary and Quaternary Systems," PhD Thesis, University of Kansas, Lawrence, Kan., 1970.
(4) Jensen, R. H., "Heterogeneous Phase Behavior of Solid Carbon Dioxide in Light Hydrocarbons at Cryogenic Temperatures," *ibid.*, 1969.
(5) Price, A. R., Kobayashi, R., *J. Chem. Eng. Data*, **4**, 40 (1959).

RECEIVED for review May 25, 1970. Accepted December 14, 1970. This project was financially supported by Grant No. GK-4193 from National Science Foundation.

Hydroxymethylabietanoic Acid and Derivatives: Dinitrile, Diamine, and Diisocyanate

KANNETH K. SUGATHAN, WILMER A. ROHDE, and GLEN W. HEDRICK[1]
Naval Stores Laboratory, Olustee, Fla. 32072

12-Hydroxymethylabietic acid is hydrogenated (nickel catalyst) to 12-hydroxymethylabietan-18-oic acid. Its conversion to 12-chloromethylabietan-18-oyl chloride and the syntheses of 12-cyanomethylabietan-18-nitrile, 12-(β-aminoethyl)abietan-18-amine, and 12-(β-isocyanatoethyl)abietan-18-isocyanate from 12-chloromethylabietan-18-oyl chloride are discussed. 12-Carboxymethylabietan-18-oic acid is readily prepared from 12-cyanomethylabietan-18-amide.

Recent efforts of the Naval Stores Laboratory and elsewhere have been directed toward making resin acid polyfunctional (*1, 4–8*). In previous research, 12-hydroxymethylabiet-7,(8)-en-18-oic acid was converted to amino alcohols, dinitriles, diamines, and diisocyanates (*10*).

In the present work, 12-hydroxymethylabietan-18-oic acid (II) was prepared by hydrogenation of 12-hydroxymethylabietic acid (I), using a nickel catalyst. A more direct route for making nitrile, amine, and isocyanate derivatives than that reported by Watson et al. (*10*) was in the conversion of II to its 12-chloromethylabietan-18-oyl chloride (V) using Vilsmeier reagent (*9*). The acid chloride was readily converted to the amide (VI). Dehydration of VI with tosyl-chloride (*10*) provided the 12-chloromethylabietan-18-nitrile (VII); reaction of VI with sodium cyanide furnished 12-cyanomethylabietan-18-amide (VIII). The dinitrile, 12-cyanomethylabietan-18-nitrile (IX), was prepared either from VII by reaction with sodium cyanide or from VIII by dehydration (*10*). The diacid (X) was made by hydrolysis of VIII. Catalytic hydrogenation of IX over cobalt produced the diamine, 12-(β-aminoethyl)abietan-18-amine

[1] To whom correspondence should be addressed.